# Nickel(II) and Iron(II) Complexes with Tetradentate NHC/Amide Hybrid Ligands

Iris Klawitter, Steffen Meyer, Serhiy Demeshko, and Franc Meyer

Institut für Anorganische Chemie, Georg-August-Universität, Tammannstraße 4, 37077 Göttingen, Germany

Reprint requests to Prof. Dr. Franc Meyer. Fax: (++49) 551 393063.
E-mail: franc.meyer@chemie.uni-goettingen.de

*Z. Naturforsch.* **2013**, *68b*, 458 – 466 / DOI: 10.5560/ZNB.2013-3091
Received March 20, 2013

*Dedicated to Professor Heinrich Nöth on the occasion of his 85$^{th}$ birthday*

Two methylene-bridged bis(imidazolium) salts $[H_4L^1](PF_6)_2$ and $[H_4L^2](PF_6)_2$ with appended amide groups have been synthesized which, after deprotonation, may serve as potentially tetradentate ligands providing two bis(imidazole-2-ylidene) and two amide donors. Using $[H_4L^1](PF_6)_2$, a square-planar nickel(II) complex $[NiL^1]$ and a six-coordinate bis(ligand) iron(II) complex $[Fe(HL^1)_2]$ have been isolated and structurally characterized. Their low-spin states have been confirmed spectroscopically, and their redox properties have been studied by cyclic voltammetry. Oxidations are metal-centered to give $Ni^{III}$ and $Fe^{III}$ species, respectively.

*Key words:* Nickel, Iron, *N*-Heterocyclic Carbene, Chelate Ligand, X-Ray Crystallography, Mößbauer Spectroscopy, Redox Properties

## Introduction

Within the last two decades, *N*-heterocyclic carbenes (NHCs) have become one of the most popular and most versatile ligand classes in organometallic chemistry, with numerous applications in homogeneous catalysis [1 – 4]. Their strong σ-donor ability as well as the inertness and the high thermodynamic stability of their complexes are among the favorable features of NHC ligands. Metal ion binding by NHCs can be further supported by introducing ancillary coordinating donor side arms at the imidazolium ring [5 – 7]. Furthermore, the linking of two or even more *N*-substituted imidazole subunits leads to multidentate NHC ligands, ranging from chelating bis(carbenes) [8] to macrocyclic tetracarbenes [9]. In view of their prevalence in catalytic applications, NHC complexes of late transition metals such as Rh and Pd are particularly abundant [10 – 13]. Recently, several group 10 metal complexes with ligands containing one or two NHC moieties and appended amide side arms have been reported (**I** [14], **II** [15], **III** [16] in Fig. 1). They were obtained by *in-situ* deprotonation of the respective imidazolium salt in the presence of a weak base or basic metal salts.

Though first examples have been described already in the 1970s [17, 18], NHC complexes of iron are still relatively scarce. They have received increasing attention only in recent years [19], spurred by possible uses in catalysis [20, 21], bioinspired chemistry [22, 23] and for the stabilization of unusual iron oxidation states [24 – 26]. A common method for synthesizing iron(II)-NHC complexes is the reaction of the respective imidazolium salts with the basic iron(II) precursor $[Fe\{Si(NMe_3)_2\}_2]_2$. Two representative examples of iron(II)-NHC complexes, namely the family of octahedrally six-coordinate complexes **IV** [27] and the square-planar tetra-coordinate complex **V** [28] (Fig. 2) all containing two chelating bis(imidazol-2-ylidene) ligands, were obtained *via* this route.

Herein we report the preparation and structural characterization of a new nickel(II) complex as well as the first iron(II) complex with potentially tetradentate amide-functionalized *N*-heterocyclic bis(carbenes) akin to the ligands used in **II** and **III**.

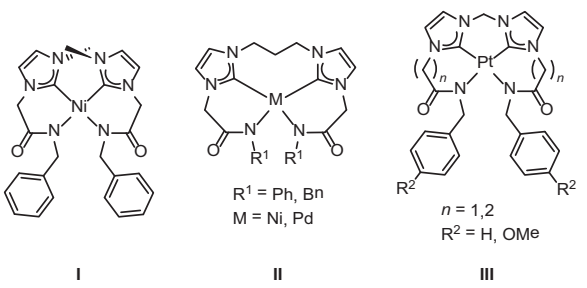


Fig. 1. Known *N*-heterocyclic bis(carbene) complexes with amide-functionalized side arms.

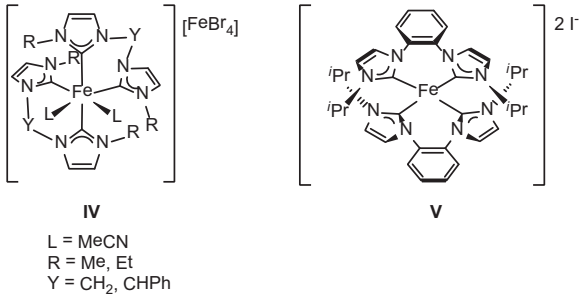


Fig. 2. Iron(II) complexes containing two *N*-heterocyclic bis(carbenes).

Their spectroscopic and electrochemical properties have been studied.

## Results and Discussion

### *Ligand synthesis*

The ligand precursors, *viz.* the amide-functionalized bis(imidazolium) salts $[H_4L^1](PF_6)_2$ and $[H_4L^2](PF_6)_2$ used in this work, were synthesized in close analogy to procedures reported previously (Scheme 1) [15, 27, 29]. To obtain $[H_4L^2](PF_6)_2$, the methylene-bridged bis(imidazole) **1** [30] was treated with the chlorinated amide **2** [31]. The parent bis(imidazolium) salt $[H_4L^1](PF_6)_2$ containing a primary amide was synthesized by linking imidazole derivative **3** [32] with dibromomethane. Because of the hygroscopic properties of both bis(imidazolium) halides, subsequent salt metathesis with potassium hexafluorophosphate is advisable and gave $[H_4L^1](PF_6)_2$ and $[H_4L^2](PF_6)_2$, which have been characterized by NMR spectroscopy, ESI mass spectrometry, and elemental analysis. $[H_4L^1](PF_6)_2$ has been used for all subsequent complexation studies.

### *Synthesis and characterization of complexes*

Conversion of the ligand precursor $[H_4L^1](PF_6)_2$ to its nickel(II) and iron(II) complexes was carried out following established procedures [15, 27]. Reaction of $[H_4L^1](PF_6)_2$ with $NiCl_2{\cdot}6\,H_2O$ at 50 °C, performed under aerobic conditions in the presence of an excess of potassium carbonate as base (Scheme 2), led to an orange solid that is moderately soluble in methanol. The product was identified as the diamagnetic neutral complex $[NiL^1]$ (**4**) containing a square-planar coordinated low-spin nickel(II) ion (see below). In contrast, treatment of $[H_4L^1](PF_6)_2$ with $[Fe\{N(SiMe_3)_2\}_2]_2$ and $KN(SiMe_3)_2$ led to a neutral octahedral complex $[Fe(HL^1)_2]$ (**5**) with two tridentate ligand strands that result from triple deprotonation of the ligand precursor $[H_4L^1](PF_6)_2$. Formation of **5** is independent of the ini-

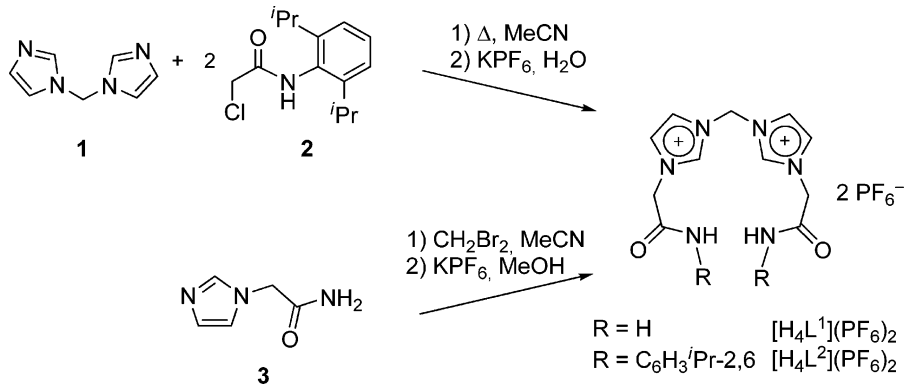


Scheme 1. Synthesis of $[H_4L^1](PF_6)_2$ and $[H_4L^2](PF_6)_2$ *via* distinct routes.

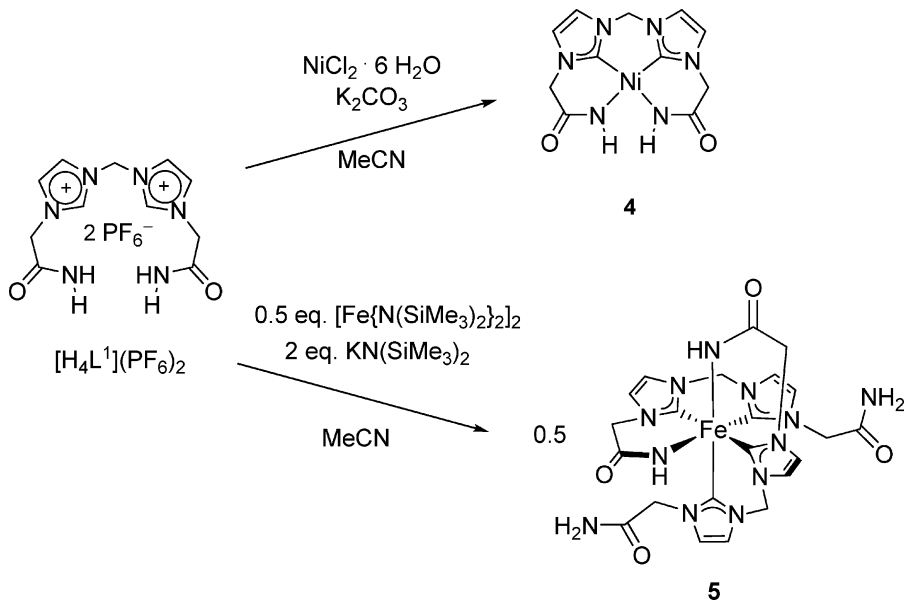


Scheme 2. Synthesis of complexes **4** and **5**.

tial ratio of $[H_4L^1](PF_6)_2$ and $[Fe\{N(SiMe_3)_2\}_2]_2$ and thus appears to be strongly favored. Both new compounds **4** and **5** were characterized by ESI mass spectrometry, cyclic voltammetry (CV) and elemental analyses.

Single crystals of complex **4**·MeOH suitable for X-ray analysis were obtained by slow diffusion of diethyl ether into a methanol solution of the crude compound. **4**·MeOH crystallizes in the monoclinic space group $P2_1/n$. The nickel ion shows a square-planar coordination (Fig. 3); selected bond lengths and angles are given in Table 1. The short Ni–$C^{NHC}$ (1.85 Å) and slightly longer Ni–$N^{amido}$ (1.90 and 1.89 Å) bonds resemble those of the known nickel(II) complexes **I** ($d = 1.85/1.92$ Å) [14] and **II** ($d = 1.89/1.94$ Å) [15]. Bond angles $C^{NHC}$–Ni–$C^{NHC}$ generally depend on whether the two NHC subunits are linked and, if so, on the length of the spacer. Nickel complexes of

Table 1. Selected bond lengths (Å) and angles (deg) of **4**.

| Bond lengths (Å) | | Angles (deg) | |
|---|---|---|---|
| Ni1–C1 | 1.8530(19) | C1–Ni1–C5 | 89.70(8) |
| Ni1–C5 | 1.8514(18) | C5–Ni1–N5 | 91.07(8) |
| Ni1–N5 | 1.8980(17) | C1–Ni1–N6 | 90.66(8) |
| Ni1–N6 | 1.8868(16) | N6–Ni1–N5 | 88.52(7) |
| | | C1–Ni1–N5 | 177.28(8) |
| | | C5–Ni1–N6 | 178.73(8) |

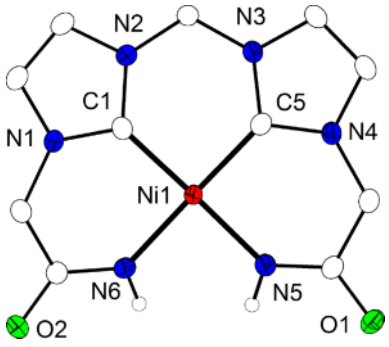


Fig. 3. ORTEP plot (30 % probability displacement ellipsoids) of **4**. C-bound hydrogen atoms and solvent molecules have been omitted for clarity.

methylene-bridged *N*-heterocyclic bis(carbenes) usually have $C^{NHC}$–Ni–$C^{NHC}$ angles in the range 83.6 to 86.6° [33–35]. In **4** this angle is almost right-angled (89.7°) as are the other bond angles at the metal ion (Table 1), reflecting the close to perfect square-planar coordination environment.

Complex **5** was initially obtained from the reaction mixture as an orange solid. The crude material proved well soluble in methanol, and deep-red crystals of **5**·4MeOH were then obtained from methanol-diethyl ether; however, these crystals were found to be only sparingly soluble in MeOH, DMF and DMSO.

Crystalline material was used for all spectroscopic and electrochemical investigations.

**5**·4MeOH crystallizes in the monoclinic space group $P2_1/c$; its molecular structure is shown in Fig. 4, and selected distances and angles are compiled in Table 2. The six-coordinate iron(II) ion is ligated by two tridentate ligand strands $[HL^1]^-$ binding in a meridional manner, and with the two amide donors in *cis* position. The remaining amide group of each ligand stays dangling. Fe–$C^{NHC}$ distances are found between 1.929 and 1.917 Å and are thus slightly shorter than in **IV** (1.916 – 1.986 Å [27]), but in the range observed for six-coordinate ferrous NHC complexes (1.91/1.96 Å [36, 37]). The Fe–$N^{amide}$ distances in **5** are 2.040 and 2.032 Å. So far, no six-coordinate iron(II) complex coordinated by two deprotonated amide groups is known. However, [*trans*-$(dmpe)_2$Fe(H)(NHCHO)] shows a very similar Fe–$N^{acetamide}$ bond length of 2.044 Å [38].

The zero-field Mößbauer spectrum of **5** at 80 K shows a quadrupole doublet with isomer shift $\delta = 0.08\ \mathrm{mm\,s^{-1}}$ and quadrupole splitting $\Delta E_Q = 1.57\ \mathrm{mm\,s^{-1}}$, which is in accordance with the presence of an octahedral low-spin (l. s., $S = 0$) iron(II). Comparison with the related six-coordinate iron(II)-NHC complex **IV** (R = Me, Y = $CH_2$, l. s., $\delta = 0.15\ \mathrm{mm\,s^{-1}}$ and $\Delta E_Q = 1.36\ \mathrm{mm\,s^{-1}}$) [27] and the square-planar compound **V** (h. s., $\delta = 0.18\ \mathrm{mm\,s^{-1}}$ and $\Delta E_Q = 4.16\ \mathrm{mm\,s^{-1}}$) [28] indicates, however, that **5** has the lowest isomer shift for iron(II) complexes with two bidentate bis(carbenes) reported so far. This likely reflects the very strong $\sigma$-donor character of all ligating groups, namely both the NHC and amide donors.

Table 2. Selected bond lengths (Å) and angles (deg) of **5**.

| Bond lengths (Å) | | Angles (deg) | |
|---|---|---|---|
| Fe1–C1 | 1.917(4) | C1–Fe1–C5 | 87.68(16) |
| Fe1–C5 | 1.918(4) | C5–Fe1–C12 | 98.46(16) |
| Fe1–C16 | 1.923(4) | C1–Fe1–N6 | 84.65(15) |
| Fe1–C12 | 1.929(4) | C12–Fe1–N12 | 84.93(15) |
| Fe1–N12 | 2.032(3) | C1–Fe1–C16 | 97.99(16) |
| Fe1–N6 | 2.040(3) | C1–Fe1–C12 | 171.56(16) |
| | | C5–Fe1–N6 | 171.68(15) |
| | | C16–Fe1–N12 | 172.30(15) |

*Electrochemical properties of the complexes*

Because of the insolubility of **4** in common organic solvents, the cyclic voltammogram (Fig. 5) was recorded in water (0.1 M $NaClO_4$). A quasi-reversible one-electron process is observed at +0.89 V *vs.* NHE and is assigned to the $[Ni^{II}L^1]/[Ni^{III}L^1]^+$ couple. The $Ni^{II}/Ni^{III}$ potential is much higher than in synthetic complexes containing $\{N_2S_2\}$ donor sets [39, 40], but comparable with redox potentials of nickel complexes of *N*-substituted cyclam derivatives [41 – 43].

To confirm that the oxidation is metal-centered and that the NHC/amide hybrid ligands remain innocent,

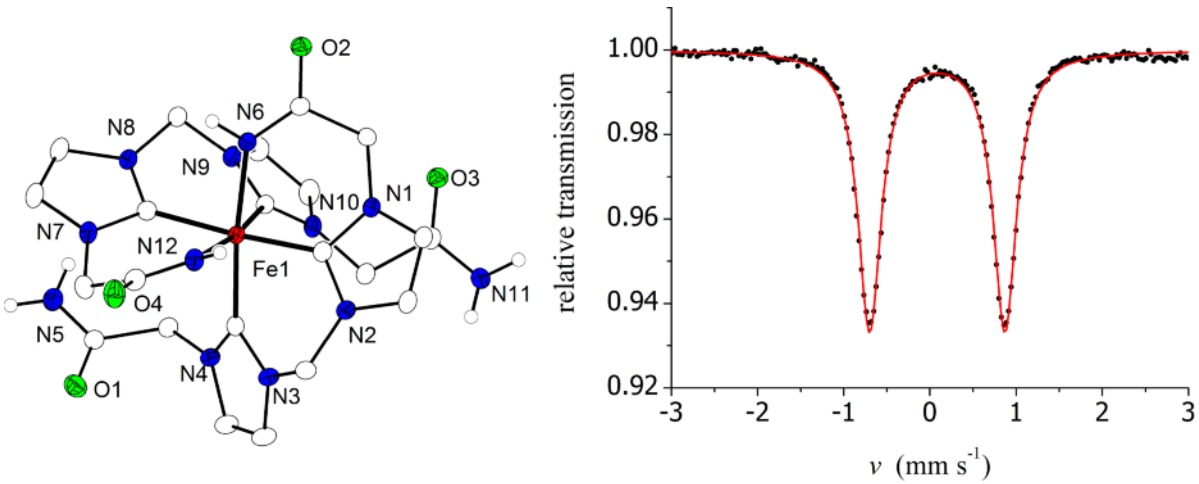


Fig. 4. Left: ORTEP plot (30 % probability displacement ellipsoids) of **5**; C-bound hydrogen atoms and solvent molecules have been omitted for clarity. Right: Zero-field Mößbauer spectrum of **5** at 80 K (natural abundance $^{57}$Fe); the solid line represents a simulation with $\delta = 0.08\ \mathrm{mm\,s^{-1}}$ and $\Delta E_Q = 1.57\ \mathrm{mm\,s^{-1}}$.

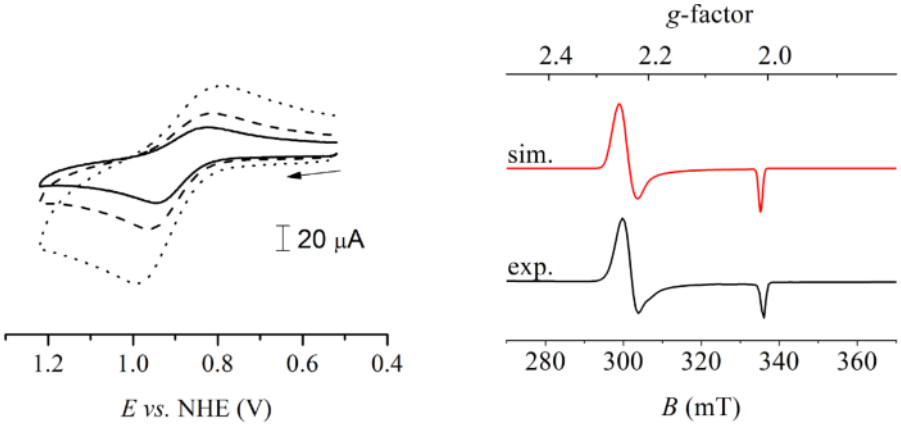


Fig. 5 (color online). Left: Cyclic voltammogram of **4** in $H_2O$ (3.0 mM, 0.1 M $NaClO_4$, 25 °C) at scan rates of 100, 200 and 500 mV $s^{-1}$; an Ag/AgCl reference electrode was used, potentials are given *vs.* NHE [44]; right: EPR spectrum of the one-electron-oxidized $[NiL^1]^+$ in frozen solution of water:glycerol (8 : 2), 0.1 M $NaClO_4$ at 140 K (black line) and simulated spectrum with $g_1 = 2.247$, $g_2 = 2.245$, $g_3 = 2.011$ (red line).

a solution of electrochemically generated $[NiL^1]^+$ in 0.1 M $NaClO_4$ water-glycerol (8 : 2) was investigated by EPR spectroscopy (sample taken after ~80% conversion). The EPR spectrum of a frozen solution at 140 K shows an almost axial spectrum with slight rhombic distortion (Fig. 5, right). Spectral simulation gives values $g_1 = 2.247$, $g_2 = 2.245$ and $g_3 = 2.011$. Such EPR signature with large anisotropy and $g_\perp > g_\parallel \approx 2.0$ is typical for a $d^7$ nickel(III) ion with the unpaired electron in the $d_{z^2}$ orbital. Any hyperfine structure is not resolved in the experimental spectrum, but including hyperfine interactions with two $^{14}N$ nuclei ($a \approx 10 \times 10^{-4}$ $cm^{-1}$) slightly improved the quality of the simulation.

The cyclic voltammogram of **5** measured in dimethylformamide (0.1 M $[nBu_4N]PF_6$) is shown in Fig. 6. A reversible one-electron redox process is observed at –0.96 V *vs.* NHE and is assigned to the $[Fe^{II}(HL^1)_2]/[Fe^{III}(HL^1)_2]^+$ couple. The value is low compared to that of a homoleptic bis[tricarbene] iron(II) complex $[(TRIS^R)_2Fe^{II}]$ ($TRIS^R$ = hydrotris(3-alkyl-imidazoline-2-yliden-1-yl)borate; R = Me, Et) synthesized by Fehlhammer *et al.* [45]. The $[(TRIS^R)_2Fe^{II}]/[(TRIS^R)_2Fe^{III}]^+$ potential was determined at around −0.7 V (value converted *vs.* NHE according to ref. [46]). The lower potential of **5** might be explained by the additional π-donor character of the two amido ligands. To confirm that the observed redox process around −0.96 V is metal-centered, a sample of **5** was oxidized chemically by addition of an excess of $AgBF_4$ in MeCN solution at 0 °C, followed by 1 h stirring and evaporation of the solvent. A zero-field Mößbauer spectrum of the resulting crude **5**$[BF_4]$, collected at 80 K, indeed shows a doublet characteristic of a low-spin iron(III) center with $\delta = 0.02$ mm $s^{-1}$ and $\Delta E_Q = 3.83$ mm $s^{-1}$. Further redox processes of **5** were observed at peak potential $E^{ox}/E^{red} = -2.25/-2.19$ V (quasi reversible) and 0.657/ 0.433 V (irreversible), but their assignment (metal- or ligand-centered) remains unclear.

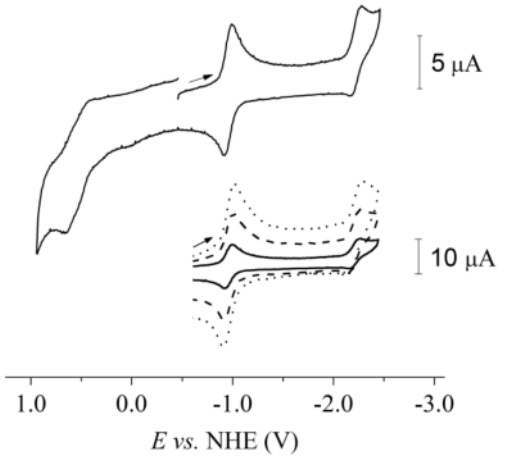


Fig. 6. Cyclic voltammogram of **5** in DMF (3.5 mM, 0.1 M $[nBu_4N]PF_6$, 25 °C) at a scan rate of 100 mV $s^{-1}$; $Fc/Fc^+$ has been used as internal standard, potentials are given *vs.* NHE [47]. The lower inset shows the wave at around −960 mV recorded at different scan rates.

## Conclusions

A nickel(II) and an iron(II) complex of a potentially tetradentate bis(imidazole-2-ylidene) ligand that bears two appended amide groups have been synthesized and structurally characterized. The combination of very strong σ-donors in the chelate scaffold, namely the two NHC and the two amide groups, enforces low-spin configurations in both cases. While the nickel(II) ion in [NiL$^1$] exhibits the anticipated square-planar coordination environment, iron(II) forms a six-coordinate bis(ligand) complex [Fe(HL$^1$)$_2$] where one amide arm of each tridentate ligand strand remains protonated and dangling. Both complexes undergo metal-centered oxidations while the NHC/amide hybrid ligands remain innocent, as was confirmed by EPR and Mößbauer spectroscopy.

## Experimental Section

All reactions and investigations of air-sensitive compounds were performed under a dry and oxygen-free nitrogen atmosphere in a glovebox (MBraun Labmaster) or by using standard Schlenck techniques. The solvents were degassed and dried according to standard methods. [Fe{Si(NMe$_3$)$_2$}$_2$]$_2$ [48], **1** [32], **2** [30], and **3** [31] were synthesized according to literature procedures. $^1$H and $^{13}$C{$^1$H} NMR spectra were recorded on Bruker Avance DRX 500 or Bruker Avance 300 spectrometers at 25 °C. Chemical shifts $\delta$ are given in ppm relative to TMS, using the residual proton signal of the solvent as internal standard. Mass spectrometry was performed with a Bruker HCT Ultra (ESI) or with a Finnigan MAT LCQ (ESI-HRMS) instrument. Melting points were determined in glass capillary tubes on a Stanford Research Systems Optimelt MPA 100 device; the values are uncorrected. Mößbauer (MB) measurements were performed with a $^{57}$Co source in a rhodium matrix using an alternating constant-acceleration Wissel Mößbauer spectrometer operated in the transmission mode and equipped with a Janis closed-cycle helium cryostat. Isomer shifts $\delta$, the quadrupole splitting $\Delta E_Q$ and full width at half maximum $\Gamma$ are given in mm s$^{-1}$. The isomer shift $\delta$ is given relative to elemental iron at ambient temperature. Simulations of the experimental data were performed with the program MFIT [49]. The EPR experiment was carried out with a Bruker ELEXSYX E500 CW-EPR-spectrometer at 140 K and X-band with spectrometer frequency 9.4349 GHz and modulation amplitude 6.0 G. Simulations were performed with the Bruker software XSOPHE [50]. Elemental analyses were carried out by the analytical laboratory of the Institute of Inorganic Chemistry at the Georg-August-University of Göttingen using an Elementar Vario EL III instrument.

### *[H$_4$L$^1$](PF$_6$)$_2$*

2-(1*H*-Imidazol-1-yl)acetamide (**3**) (751 mg, 6.0 mmol, 2.0 eq.) and dibromomethane (0.21 mL, 3.0 mmol, 1.0 eq.) were dissolved in MeCN (50 mL) and the reaction mixture stirred at 110 °C in a 100 mL ACE Glass autoclave for 3 days. The resulting precipitate was separated by filtration and then dissolved in MeOH (5 mL). $KPF_6$ (1.66 g, 9.0 mmol 3.0 eq.) was added and the reaction mixture was stirred for 1 h. The product [H$_4$L$^1$](PF$_6$)$_2$ (1.08 g, 1.95 mmol, 65 %) was filtered off and washed with MeOH; m. p. 169 °C (decomp.). – $^1$H NMR (300 MHz, [D$_6$]DMSO, 25 °C): $\delta$ = 9.41 (broad s, 2H, H$^{2\text{-Im}}$), 7.96 (broad s, 2H, H$^{\text{Im}}$), 7.59 (s, 2H, NH), 7.80 (broad s, 2H, H$^{\text{Im}}$), 7.59 (s, 2H, NH), 6.71 (s, 2H, CH$_2$), 5.02 (s, 4H, CH$_2$). – $^{13}$C NMR (75 MHz, [D$_6$]DMSO, 25 °C): $\delta$ = 166.4 (CO), 138.8 (C$^{2\text{-Im}}$), 125.0 (C$^{\text{Im}}$), 121.5 (C$^{\text{Im}}$), 58.5 (NCH$_2$N), 50.9 (CH$_2$). – MS ((+)-ESI, MeOH): $m/z$(%) = 132 (100) [H$_4$L]$^{2+}$, 263 (15) [H$_3$L]$^+$. – HRMS ((+)-ESI, MeOH): $m/z$ = 132.0662 (calcd. 132.0662 for [C$_{11}$H$_{16}$N$_6$O$_2$]$^{2+}$), 409.0971 (calcd. 409.0972 for [C$_{11}$H$_{16}$N$_6$O$_2$PF$_6$]$^+$). – IR (KBr): $\nu$ (cm$^{-1}$) = 419 (m), 560 (s) 605 (m), 752 (m), 831 (s), 1014 (w), 1164 (w), 1163 (s), 1315 (m), 1397 (s), 1682 (s), 3093 (s), 3346 (s).

### *[H$_4$L$^2$](PF$_6$)$_2$*

Bis(imidazol-1-yl)methane (**1**) (223 mg, 1.5 mmol, 1.0 eq.) and 2-chloro-*N*-(2,6-diisopropylphenyl)acetamide (**2**) (761 mg, 3.0 mmol, 2.0 eq.) were dissolved in MeCN (50 mL) and the reaction mixture stirred at 110 °C in a 100 mL ACE Glass autoclave for 3 days. The resulting precipitate was separated by filtration and then dissolved in water (20 mL). $KPF_6$ (828 mg, 4.5 mmol, 3.0 eq.) was added, and the resulting mixture was stirred for 1 h. The product precipitated from the reaction mixture. Separation by filtration and the removal of the solvents under reduced pressure at 150 °C afforded [H$_4$L$^2$](PF$_6$)$_2$. (1.14 g, 1.3 mmol, 87 %) as a colorless solid; m. p. ∼ 180 – 185 °C (decomp.). – $^1$H NMR (300 MHz, [D$_6$]DMSO, 25 °C): $\delta$ = 9.88 (s, 2H, NH), 9.57 (s, 2H, H$^{\text{Im2}}$), 8.05 (s, 2H, H$^{\text{Im}}$), 7.88 (s, 2H, H$^{\text{Im}}$), 7.20 – 7.32 (m, 6H, H$^{\text{Ar}}$), 6.81 (s, 2H, CH$_2$), 5.43 (s, 4H, CH$_2$), 3.08 (sept, $^3J_{\text{HH}}$ = 6.7 Hz, 4H, CH), 1.13 (broad s, 24H, CH$_3$). – $^{13}$C NMR (75 MHz, [D$_6$]DMSO, 25 °C): $\delta$ = 164.4 (CO), 146.0 (C$^{\text{Ar}}$), 138.9 (C$^{2\text{-Im}}$), 131.2 (C$^{\text{Ar}}$), 128.2 (C$^{\text{Ar}}$), 124.9 (C$^{\text{Im}}$), 123.2 (C$^{\text{Ar}}$), 121.8 (C$^{\text{Im}}$), 58.6 (NCH$_2$N), 50.9 (CH$_2$), 28.04 (CH), 23.9 (CH$_3$), 23.4 (CH$_3$). – MS ((+)-ESI, MeCN): $m/z$(%) = 292 (100), [H$_4$L]$^{2+}$, 729 (9), [H$_4$L(PF$_6$)]$^+$. – HRMS ((+)-ESI, MeOH): $m/z$ = 292.1914 (calcd. 292.1914 for [C$_{35}$H$_{48}$N$_6$O$_{22}$]$^+$), 729.3470 (calcd. 729.3475 for [C$_{35}$H$_{48}$N$_6$O$_2$PF$_6$]$^+$). – IR (KBr): $\nu$ (cm$^{-1}$) = 558 (s), 849 (s), 1172 (s), 1240 (m) 1365 (m), 1445 (m), 1523 (s), 1689

(s), 2342 (w), 2361 (w), 2872 (m), 2970 (s), 3168 (m), 3392 (m), 3645 (m).

*Complex **4***

$NiCl_2 \cdot 6\,H_2O$ (86 mg, 0.36 mmol, 1.0 eq.) and $K_2CO_3$ (200 mg, 0.72 mmol, 4.0 eq.) were added to a solution of $[H_4L^1](PF_6)_2$ (200 mg, 0.36 mmol, 1.0 eq.) in MeOH (25 mL) and the mixture was stirred at 50 °C for 5 h. After cooling to room temperature diethyl ether (100 mL) was added. The resulting precipitate was separated by filtration and recrystallized from water to give **4** as orange crystals (81 mg, 0.226 mmol, 71 %). – $^1$H NMR (300 MHz, $D_2O$, 25 °C): $\delta = 7.38$ (broad s, 2H, $H^{Im}$), 7.24 (broad s, 2H, $H^{Im}$), 6.18 (broad s, 2H, $CH_2$), 4.46 (s, 4H, $CH_2$). – $^{13}$C NMR (75 MHz, $D_2O$, 25 °C): $\delta$ = 171.9 (CO), 157.4 (NHC), 122.8 ($C^{Im}$), 120.7 ($C^{Im}$), 61.8 ($NCH_2N$), 51.2 ($CH_2$). – MS ((+)-ESI, MeOH): $m/z$ (%) = 357.0 (100) $[M+K]^+$, 279.1 (63), 341.0 (55) $[M+Na]^+$, 319.0 (32) $[M+H]^+$. – HRMS ((+)-ESI, MeOH): $m/z$ = 319.0450 (calcd. 319.0448 for $[C_{11}H_{13}N_6NiO_2]^+$). – IR (KBr) $\nu$ ($cm^{-1}$) = 664 (w), 727 (w), 831 (s), 1031 (w), 1175 (w), 1279 (s), 1330 (s), 1430 (s), 1445 (s), 1580 (vs), 1618 (vs), 3085 (s), 3115 (s), 3167 (s), 3253 (s), 3467 (s). – Elemental analysis (%) for $C_{11}H_{12}N_6NiO_2 \cdot {}^1/_2\,H_2O$: calcd. C 40.29, H 4.00, N 25.63; found C 39.40, H 3.61, N 25.30.

*Complex **5***

$[Fe\{N(SiMe_3)_2\}_2]_2$ (75 mg, 0.2 mmol, 1.0 eq.) was added to a solution of $[H_4L^1](PF)_6$ (222 mg, 0.4 mmol, 2.0 eq.) in acetonitrile (5 mL) and the reaction mixture stirred for 30 min. After the addition of $KN(SiMe_3)_2$ (239 mg, 1.2 mmol, 4.0 eq.) the suspension was stirred for further 15 h. The resulting precipitate was separated by filtration and dissolved in methanol (5 mL). Addition of diethyl ether (20 mL) led to the gradual formation of red crystals of $[Fe(HL^1)_2]$ (**5** · 4 MeOH; 59 mg, 0.08 mmol, 42 %). – MS ((+)-ESI, MeOH): $m/z$(%) = 578.2 (100) $[M]^+$, 615.2 (19). – HRMS ((+)-ESI, MeOH): $m/z$ = 578.1538 (calcd. 578.1549 for $[C_{22}H_{26}FeN_{12}O_4]^+$). – IR (KBr): $\nu$ ($cm^{-1}$) = 736 (w) 834 (w), 1216 (w), 1288 (w), 1339 (w), 1403 (s), 1430 (s), 1545 (vs), 1574 (vs), 1686 (vs), 3428 (vs). – MB: $\delta$ = 0.08 mm $s^{-1}$, $\Delta E_Q$ = 1.57 mm $s^{-1}$. – Elemental analysis (%) for $C_{22}H_{26}FeN_{12}O_4 \cdot$ 2 $CH_3OH$: calcd. C 44.78, H 5.33, N 26.16; found C 44.38, H 4.86, N 26.67. Two of the MeOH solvent molecules included in the crystal lattice of **5** · 4 MeOH are obviously lost upon drying the sample for elemental analysis.

*X-Ray structure determinations*

X-Ray data were collected on a Stoe IPDS II diffractometer (graphite-monochromatized Mo$K_\alpha$ radiation, $\lambda$ = 0.71073 Å) by use of $\omega$ scans at –140 °C. Face-indexed absorption corrections were performed numerically with the program X-RED [51]. The structures were solved by Direct Methods and refined on $F^2$ using all reflections with SHELXS/L-97 [52]. Non-hydrogen atoms were refined anisotropically. Most hydrogen atoms were placed in calculated positions and assigned to an isotropic displacement parameter of 1.2 / 1.5 $U_{eq}$(C/O). The positional and isotropic thermal parameters of the oxygen- or nitrogen-bound hydro-

Table 3. Crystal structure data for **4** and **5**.

| | **4** | **5** |
|---|---|---|
| Formula | $C_{12}\,H_{16}\,N_6\,Ni\,O_3$ | $C_{26}\,H_{42}\,Fe\,N_{12}\,O_8$ |
| $M_r$ | 351.02 | 706.57 |
| Crystal size, $mm^3$ | 0.40 × 0.26 × 0.24 | 0.22 × 0.18 × 0.12 |
| Crystal system | monoclinic | monoclinic |
| Space group | $P2_1/n$ | $P2_1/c$ |
| $a$, Å | 13.5849(12) | 9.6387(4) |
| $b$, Å | 7.3581(4) | 16.1749(11) |
| $c$, Å | 13.8679(13) | 21.3184(10) |
| $\beta$, deg | 101.535(7) | 95.244(4) |
| $V$, Å$^3$ | 1358.22(19) | 3309.7(3) |
| $Z$ | 4 | 4 |
| $D_{calcd.}$, g $cm^{-3}$ | 1.72 | 1.42 |
| $\mu$(Mo$K_\alpha$), $cm^{-1}$ | 1.5 | 0.5 |
| $F$(000), e | 728 | 1488 |
| *hkl* range | ±17, −7 to 9, ±17 | −11 to 12, ±20, ±26 |
| Refl. measd / unique / $R_{int}$ | 10847 / 2866 / 0.0565 | 28695 / 7040 / 0.0962 |
| Param. refined | 212 | 456 |
| $R(F)$ [$F > 4\,\sigma(F)$] | 0.0290 | 0.0729 |
| $wR(F^2)$ (all data) | 0.0815 | 0.1651 |
| GoF ($F^2$) | 1.064 | 1.069 |
| $\Delta\rho_{fin}$ (max / min), e Å$^{-3}$ | 0.694 / −0.441 | 0.664 / −0.417 |

gen atoms were refined without any restraints or constraints in case of **4**·MeOH, in case of **5**·4MeOH only nitrogen-bound hydrogen atoms. Crystal data and details of the data collections and structure refinements are given in Table 3.

CCDC 926872 and 926873 contain the supplementary crystallographic data for this paper. These data can be obtained free of charge from The Cambridge Crystallographic Data Centre *via* www.ccdc.cam.ac.uk/data_request/cif.

*Acknowledgement*

Financial support by the Georg-August-University Göttingen is gratefully acknowledged. We thank Dr. A. C. Stückl for measuring the EPR spectrum, J. Teichgräber for CV measurements, and Dr. H. Frauendorf (Institute for Organic and Biomolecular Chemistry, Georg-August-University Göttingen) for collecting HRMS spectra.

[1] W. A. Herrmann, *Angew. Chem. Int. Ed.* **2002**, *41*, 1290 – 1309.
[2] C. G. Fortman, S. P. Nolan, *Chem. Soc. Rev.* **2011**, *40*, 5151 – 5169.
[3] A. Correa, S. P. Nolan, L. Cavallo, *Top. Curr. Chem.* **2011**, *302*, 131 – 155.
[4] A. Kumar, P. Ghosh, *Eur. J. Inorg. Chem.* **2012**, 3955 – 3969.
[5] O. Kühl, *Chem. Soc. Rev.* **2007**, *36*, 592 – 607.
[6] A. John, P. Ghosh, *Dalton Trans.* **2010**, *39*, 7183 – 7206.
[7] D. Yuan, H. V. Huynh, *Molecules* **2012**, *17*, 2491 – 2517.
[8] M. Poyatos, J. A. Mata, E. Peris, *Chem. Rev.* **2009**, *109*, 3677 – 3707.
[9] P. G. Edwards, F. E. Hahn, *Dalton Trans.* **2011**, *40*, 10278 – 10288.
[10] A. T. Normand, K. J. Cavell, *RSC Catalysis Series (N-Heterocyclic Carbenes)*, **2011**, *6*, 252 – 283.
[11] J. A. Zata, M. Poyatos, *Current Org. Chem.* **2011**, *15*, 3309 – 3324.
[12] A. R. Almeida, A. F. Peixoto, M. J. F. Calvete, M. P. M. P. Gois, P. M. M. Pereira, *Current Org. Synth.* **2011**, *8*, 764 – 775.
[13] S. Budagumpi, R. A. Haque, A. W. Salman, *Coord. Chem. Rev.* **2012**, *256*, 1787 – 1830.
[14] S. Kumar, A. Narayanan, M. N. Rao, M. M. Shaikh P. Ghosh, *J. Organomet. Chem.* **2012**, *696*, 4159 – 4165.
[15] F. Jean-Baptiste dit Dominique, H. Gornitzka, C. Hemmert, *Organometallics* **2010**, *29*, 2868 – 2873.
[16] Y. Unger, T. Strassner, *J. Organomet. Chem.* **2012**, *713*, 203 – 208.
[17] K. Öfele, C. G. Kreiter, *Chem. Ber.* **1972**, *105*, 529 – 540.
[18] G. Huttner, W. Gartzke, *Chem. Ber.* **1972**, *105*, 2714 – 2725.
[19] M. J. Ingleson, R. A. Layfield, *Chem. Commun.* **2012**, *48*, 3579 – 3589.
[20] L. Delaude, A. Demonceau, *RSC Catalysis Series* **2011**, *6*, 196 – 227.
[21] D. Bézier, J.-B. Sortais, C. Darcel, *Adv. Synth. Catal.* **2013**, *355*, 19 – 33.
[22] D. Morvan, J.-F. Capon, F. Gloaguen, A. Le Goff, M. Marchivie, F. Michaud, P. Schollhammer, J. Talarmin, J.-J. Yaouanc, R. Pichon, N. Kervarec, *Organometallics* **2007**, *26*, 2042 – 2052.
[23] L. Deng, R. H. Holm, *J. Am. Chem. Soc.* **2008**, *130*, 9878 – 9886.
[24] C. Vogel, F. W. Heinemann, J. Sutter, C. Anthon, K. Meyer, *Angew. Chem. Int. Ed.* **2008**, *47*, 2681 – 2684.
[25] J. J. Scepaniak, C. S. Vogel, M. M. Khusniyarov, F. W. Heinemann, K. Meyer, J. M. Smith, *Science* **2011**, *331*, 1049 – 1052.
[26] S. Meyer, I. Klawitter, S. Demeshko, E. Bill, F. Meyer, *Angew. Chem. Int. Ed.* **2013**, *52*, 901 – 905.
[27] S. Meyer, C. M. Orben, S. Demeshko, S. Dechert, F. Meyer, *Organometallics* **2011**, *30*, 6692 – 6702.
[28] S. Zlatogorsky, C. A. Muryn, F. Tuna, D. J. Evans, M. J. Ingleson, *Organometallics* **2011**, *30*, 4974 – 4982.
[29] T. Scherg, S. K. Schneider, G. D. Frey, J. Schwarz, E. Herdtweck, W. A. Herrmann, *Synlett* **2006**, 2894 – 2907.
[30] E. Díez-Barra, A. de la Hoz, A. Sánchez-Migallón, J. Tejeda, *Heterocycles* **1992**, *34*, 1365 – 1373.
[31] R. M. Thomas, B. K. Keitz, T. M. Champagne, R. H. Grubbs, *J. Am. Chem. Soc.* **2011**, *133*, 7490 – 7496.
[32] R. J. Sundberg, D. C. Mente, I. Yilmaz, G. Gupta, *J. Heterocyclic Chem.* **1977**, *14*, 1279 – 1281.
[33] R. E. Douthwaite, D. Häussinger, M. L. H. Green, P. J. Silock, *Organometallics* **1999**, *18*, 4582 – 4590.
[34] Z. Xi, X. Zhang. W. Chen, S. Fu, D. Wang, *Organometallics* **2007**, *26*, 6636 – 6642.
[35] W. A. Hermann, J. Schwarz, M. G. Gardinger, M. Spiegeler, *J. Organomet. Chem.* **1999**, *575*, 80 – 86.
[36] D. S. McGuinnes, V. C. Gibson, J. W. Steed, *Organometallics* **2004**, *23*, 6288 – 6292.
[37] O. Kaufhold, F. E. Hahn, T. Pape, A. Hepp, *J. Organomet. Chem.* **2008**, *693*, 3435 – 3440.
[38] D. J. Fox, R. G. Bergmann, *J. Am. Chem. Soc.* **2003**, *125*, 8984 – 8985.

[39] J. Shearer, N. Zhao, *Inorg. Chem.* **2006**, *45*, 9637 – 9639.
[40] H.-J. Krüger, G. Pang, R. H. Holm, *Inorg. Chem.* **1991**, *30*, 734 – 742.
[41] E. K. Barefield, G. M. Freeman, D. G. van Derveer, *Inorg. Chem.* **1986**, *25*, 552 – 558.
[42] G. Nirmala, A. K. Rahiman, S. Sreedaran, R. Jagadeesh, N. Raaman, V. Narayanan, *J. Mol. Struct.* **2011**, *989*, 91 – 100.
[43] F. Meyer, H. Kozlowski in *Comprehensive Coordination Chemistry II* (Eds.: J. A. McCleverty, T. J. Meyer), Vol. 6, Elsevier, Oxford **2004**, pp. 247 – 554.
[44] R. G. Bates, J. B. Macaskill, *Pure & Appl. Chem.* **1978**, *50*, 1701 – 1706.
[45] R. Fränkel, U. Kernbach, M. Bakola-Christianopoulou, U. Plaia, M. Suter, W. Ponikwar, H. Nöth, C. Moinet, W. P. Fehlhammer, *J. Organomet. Chem.* **2001**, *617 – 618*, 530 – 545.
[46] V. V. Pavlishchuk, A. W. Addison, *Inorg. Chim. Acta* **2000**, *298*, 97 – 102.
[47] J. R. Aranzaes, M.-C. Daniel, D. Astruc, *Can. J. Chem.* **2006**, *84*, 288 – 299.
[48] R. A. Andersen, K. Faergri, J. C. Green, A. Haaland, M. F. Lappert, W.-P. Leung, K. Rypdal, *Inorg. Chem.* **1988**, *27*, 1782 – 1786.
[49] E. Bill, MFIT, Max-Planck Institute for Bioinorganic Chemistry, Mülheim/Ruhr (Germany).
[50] G. R. Hanson, K. E. Gates, C. J. Noble, M. Griffin, A. Mitchell, S. Benson, *J. Inorg. Biochem.* **2004**, *98*, 903 – 916.
[51] X-RED, Stoe & Cie GmbH, Darmstadt (Germany) **2002**.
[52] G. M. Sheldrick, *Acta Crystallogr.* **2008**, *A64*, 112 – 122.